holds special significance in the desert Basin and Range province, where low water tables may limit the surface discharge of hot water and/or steam. In remote desert areas, these thermal zones may be detected most easily with remote TIR sensing methods. A preliminary study using 5-channel TIMS data has shown that appropriate correction for topographic slope orientation, albedo, and thermal inertia can increase the number of remotely detected thermal anomalies by an order of magnitude (Coolbaugh et al. 2000). This initial study was performed in the Steamboat Springs region. Similar work with ASTER data is being conducted over the Brady Hot Springs region (Figure 1), where a thermal anomaly associated with the Brady's fault (white area near the center of the image) shows up clearly on raw imagery. At 90m/pixel this spaceborne data can easily identify a thermal feature ~2km in length. We will present the methodology of the approach and final analysis of the ASTER scenes at the meeting. In the summer of 2002, we hope to acquire day/night pairs at much higher spatial resolution than ASTER; preliminary analysis of these data will be included.

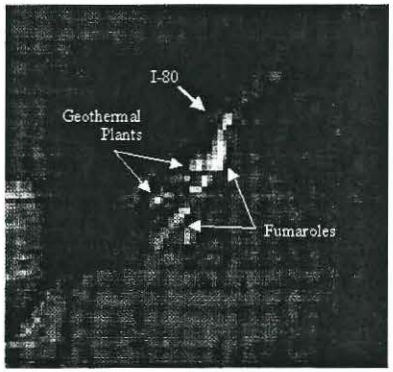

Hyperspectral Mineral Mapping

Mineral mapping using the SEBASS data has been the subject of several years of work in calibration and field validation of the data set (Vaughan, *et. al.*, submitted). The advantage of hyperspectral thermal imagery is that individual minerals can clearly be identified and mapped at the 2m spatial scale. The thermal wavelengths can also distinguish a number of primary silicates (feldspars, quartz, opaline silica) that are spectrally bland or have features that are non-unique at shorter wavelengths. We have worked with SEBASS data over an older pit and vent structure where elemental sulfur is exposed in the field, as well as the main Steamboat terrace. Clearly distinguished are a number of silicate deposits with varying compositions. Over the main sinter terrace SEBASS has distinguished younger from older sinter based on the strength of the absorption features. Our analysis shows the hyperspectral SEBASS data have the ability to map lithologies based on subtle spectral variations in mineralogy. Even a simple method such as a decorrelation stretch (Gillespie, *et. al.*, 1986) can clearly separate quartz, clay and feldspar regions with intermediate colors suggesting sulfates such as jarosite or alunite. Detailed spectral mapping discriminates pure quartz from quartz/alunite, clays including kaolinite, montmorillonite and illite, varying ages of sinter deposits, and a variety of sulfates such as gypsum, alunite and jarosite. We will present initial mineral maps for the Steamboat region as well as a site characterization using a multi-spectral instrument with a broader swath than SEBASS. We should acquire short wavelength hyperspectral data this summer for synthesis with the SEBASS data.

Summary

It is expected that this work will help identify new methods of remote characterization of geothermal site potential. It is hoped that unique mineral indicators of springs or seeps (salts, borates), levels of vegetation stress and/or thermal anomalies can be used to target new sites or assist in identifying expansion in existing areas.

Acknowledgments

This material is based upon work supported by the U.S. Department of Energy under instrument number DE-FG07-02ID14311.

References

Allis, R. G., Nash, G., and Johnson, S. D., Conversion of thermal infrared surveys to heat flow: comparisons from Dixie Valley, Nevada, and Wairakei, New Zealand; *Geothermal Resources Council Trans*, 23, p. 499-504, 1999.

Coolbaugh, M. F., Taranik, J. V., and Kruse, F. A., Mapping of surface geothermal anomalies at Steamboat Springs, NV. using NASA Thermal Infrared Multispectral Scanner (TIMS) and Advanced Visible and Infrared Imaging Spectrometer (AVIRIS) data; *In:* Proceedings, 14th Thematic Conference, Applied Geologic Remote Sensing, Environmental Research Institute of Michigan (ERIM), Ann Arbor, MI., p. 623-630, 2000.

Gillespie, A.R., A.B. Kahle, and R.E. Walker, Color enhancement of highly correlated images. I. Decorrelation and HIS contrast stretches, *Remote Sensing of Environment*, 44, p. 165-178, 1986.

King, T.V.V., R.N. Clark, and G.A. Swayze, Applications of imaging spectroscopy data: A case study at Summitville, Colorado, in *Remote Sensing for Site Characterization*, F. Kuehn et al. Eds., Springer-Verlag, pp.164-185, 2000.

Kruse, F.A. Visible-Infrared sensors and case studies, in *Remote Sensing for the Earth Sciences: Manual of Remote Sensing, 3rd Ed., Vol. 3*, A. N. Rencz, Ed., pp. 567-611, 1999.

Lee, K., Analysis of thermal infrared imagery of the Black Rock Desert geothermal area; *Colo. Sch. Mines Quarterly*, n. 3, part 1, p. 31-43, 1978.

Vaughan, R.G., W.M. Calvin and J.V. Taranik, SEBASS hyperspectral thermal infrared data: Calibrated surface emissivity and mineral mapping, *Remote Sensing of Environment*, submitted, April 2002.

A Geothermal GIS for Nevada: Defining Regional Controls And Favorable Exploration Terrains for Extensional Geothermal Systems

Mark F. Coolbaugh[1], James V. Taranik[1], Gary L. Raines[2], Lisa A. Shevenell[3], Don L. Sawatzky[3], Richard Bedell[3] and Timothy B. Minor[4]

[1]Great Basin Center for Geothermal Energy, University of Nevada, Reno, NV. USA 89557
[2]United States Geological Survey, Reno Office, University of Nevada, Reno, NV. USA 89557
[3]Great Basin Center for Geothermal Energy, University of Nevada, Reno, NV. USA 89557
[4]Desert Research Institute, 2215 Raggio Parkway, Reno, NV. USA 89512-1095

Keywords

Geothermal, GIS, Nevada, Great Basin, geochemistry, extensional, structure

ABSTRACT

Spatial analysis with a GIS was used to evaluate geothermal systems in Nevada using digital maps of geology, heat flow, young faults, young volcanism, depth to groundwater, groundwater geochemistry, earthquakes, and gravity. High-temperature (>160°C) extensional geothermal systems are preferentially associated with northeast-striking late Pleistocene and younger faults, caused by crustal extension, which in most of Nevada is currently oriented northwesterly (as measured by GPS). The distribution of sparse young (<1.5Ma) basaltic vents also correlate with geothermal systems, possibly because the vents help identify which young structures penetrate deeply into the crust. As expected, elevated concentrations of boron and lithium in groundwater were found to be favorable indicators of geothermal activity.

Known high-temperature (>160°C) geothermal systems in Nevada are more likely to occur in areas where the groundwater table is shallow (<30m). Undiscovered geothermal systems may occur where groundwater levels are deeper and hot springs do not issue at the surface. A logistic regression exploration model was developed for geothermal systems, using young faults, young volcanics, positive gravity anomalies, and earthquakes to predict areas where deeper groundwater tables are most likely to conceal geothermal systems.

Introduction

Two types of high-temperature geothermal systems are recognized in the Great Basin: the "magmatic-type," which occur on the margins of the Great Basin (e.g., Long Valley caldera), and the "extensional-type," which are "amagmatic" and occur within the interior (e.g., Dixie Valley; Koenig and McNitt, 1983; Wisian, *et. al.*, 1999). Because Nevada is almost exclusively located within the interior of the Great Basin, a study of geothermal systems in Nevada constitutes a study of extensional-type systems, to the exclusion of the magmatic type.

The locations of magmatic-type geothermal systems are relatively easy to predict because of their close spatial relationship with young silicic volcanics (Koenig and McNitt, 1983). In contrast, exploration for extensional-type systems is more difficult because they lack a clear volcanic association. In this study, a geographic information system (GIS) was used to integrate disparate types of geologic, chemical, and physical data to predict where extensional geothermal systems are most likely to occur in Nevada.

Background

The temperatures of extensional systems in Nevada can be high (locally exceeding 200°C): this has been linked to the presence of high crustal heat flow in the Great Basin (related to a thin crust) and active extensional faulting, which allows meteoric fluids to penetrate deeply into the crust and be heated to high temperatures (e.g., Wisian, *et. al.*, 1999). This suggests favorable environments for geothermal systems could be defined using maps of heat-flow and young structure. However, the very regional character of most heat flow data limits its predictive capability. Similarly, the distribution of young faults is an imperfect indicator of geothermal potential because many young faults aren't recognizable or haven't been mapped on the surface. Furthermore, a map of young faults by itself won't necessarily indicate which faults provide open pathways for geothermal fluids.

Additional evidence can improve the models. In the current study, earthquake maps, young basaltic vents, and GPS-based geodetic measurements of crustal extension are used to help identify which young faults are most likely to form open conduits for fluid flow. Maps of the groundwater table depth are used to identify possible geothermal areas where surface manifestations of geothermal activity, such as hot springs and fumaroles, may not be present. Groundwater geochemical anomalies provided direct evidence of proximity to a geothermal sys-

tem. The influence of deep carbonate aquifers on geothermal potential is also assessed.

Methodology

The geothermal GIS was constructed using ArcView GIS v.3.2a software (Raines, *et. al.*, 2000). Spatial analysis was performed with Arc-SDM, a spatial data-modeling package developed by the Geological Survey of Canada (GSC) and the United States Geological Survey (USGS; Kemp, *et. al.*, 2001).

The spatial analysis consisted of three main stages; 1) selection of training points (known hot springs and geothermal systems), 2) analysis of correlation between training sites and evidence layers (i.e., maps of heat flux, young faults, etc.), and 3) integration of evidence layers into a predictive model to locate geothermal systems. Correlations between maps and geothermal systems were evaluated using the weights-of-evidence method, which is based on Bayes' Rule of Probability (Bonham-Carter, 1996, ch. 9). Weights-of-evidence uses several data-driven statistics, including positive weights, negative weights, and contrast (e.g., Raines, *et. al.*, 2000). After statistical optimization, the evidence layers were integrated together using logistic regression to produce maps predicting geothermal favorability. Logistic-regression is a binary form of multiple-regression that does not require conditional independence of data (Wright, 1996, p. 140-146).

Sources of Data

Training sites were compiled largely from databases of the Nevada Bureau of Mines and Geology (NBMG; Garside, 1994; Shevenell, *et. al.*, 2000) and a western U.S. geothermal database maintained at Southern Methodist University (SMU; http://www2.smu.edu/geothermal/). Digital maps of Quaternary faults (Singer, 1996) and radiometric age dates were provided by Raines, *et. al.*, (1996). Groundwater chemistry and depth to water table data were obtained from the USGS National Water Information System (NWIS) database at: *http://water.usgs.gov/nv/nwis*. A digital map of regional heat flux for the western U.S. was provided by David Blackwell of SMU. Maps of Paleozoic carbonate rocks (projected beneath Cenozoic cover) and isostatic gravity were obtained from the NBMG web site at: *ftp://ftp.nbmg.unr.edu/NBMG/ofr962/index.htm* (Singer, 1996). Earthquake catalogs were downloaded from the Nevada Seismological Laboratory and interpreted with the assistance of Diane DePolo (*http://www.seismo.unr.edu/ftp/pub/catalog/*).

Space limitations do not permit a full discussion of database processing techniques, but questions can be directed to the primary author. Color versions for the figures shown in this paper, and additional figures, can be found on the Great Basin Center for Geothermal Energy (GBCGE) web site at *http://www.unr.edu/geothermal/meetingsandpresentations/meetings_pres.html*

Training Points

Geothermal training sites were grouped into four main categories: high temperature (>160°C, 20 sites), medium temperature (100-160°C, 39 sites), low temperature (70-100°C, 48 sites), and warm (37-70°C, 53 sites). The temperature assigned to each geothermal system was equal to the greater of 1) the maximum measured temperature, or 2) the average temperature calculated from geothermometers. A fifth non-exclusive geothermal category called "power" was also created, consisting of geothermal systems currently producing electrical power (Shevenell, *et. al.*, 2000) plus sub-economic geothermal systems that have produced at least some high-temperature flow as defined by Edmiston and Benoit (1984).

Geothermometer calculations were employed in this study to reduce bias caused by the fact that not all geothermal systems have been drilled and sampled below the surface. Such calculations are subject to error, especially when the waters sampled are at relatively low temperatures. Geothermometer-based temperature estimates for high-temperature systems were taken from Mariner, *et. al.*, (1983). Because Mariner's report does not include data from lower-temperature systems or hot springs from the southern part of the state, additional temperatures were calculated using chemical analyses from Garside (1994). The difference between the SiO_2 and Mg-corrected Na-K-Ca temperature estimates in the NBMG database averaged 14%.

In selecting geothermal systems to be used as training sites for modeling, a minimum separation distance of 10 kilometers was imposed to prevent using wells or springs from the same geothermal system twice. Some locations in the NBMG database come from deep oil exploration wells. If the temperatures encountered in those wells did not exceed the regional geothermal gradient, those wells were not included.

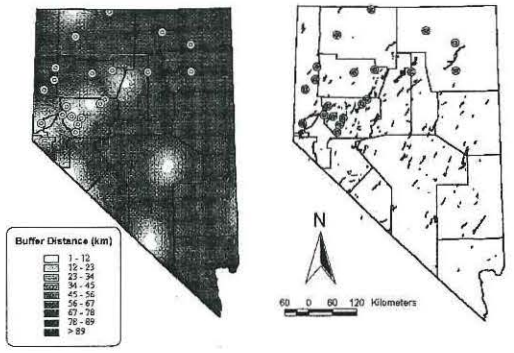

Figure 1. Distribution of high temperature (>160°C) geothermal systems (double circles) relative to (a) buffer distance to the nearest volcanic vent (<1.5Ma), and (b) northeast-striking faults (azimuths of 17-107 deg.) of late Pleistocene and younger age.

Analysis Of Evidence Layers

Young Volcanics

Although most Quaternary volcanism in the Great Basin occurs along it's margins (Blackwell, 1983), sparse basaltic volcanism is distributed in the interior (Figure 1a). A rough visual correlation between volcanism ≤1.5 Ma and high-temperature geothermal systems can be observed in Figure 1a, but a statistical plot (Figure 2) helps quantify the degree of correlation. Higher-temperature groupings of geothermal systems show higher correlation, as measured by the weights-of-evidence contrast. The highest contrasts, for geothermal systems located less than 10 km from a young volcanic vent, suggest that in some instances vent-related structural conduits provide flow paths for geothermal fluids. High-temperature (>160°C) and "power"-type geothermal systems show relatively high contrast at greater distances, as much as 75 kilometers from the vents. For example, "power" geothermal systems occur more frequently in areas where the distance to a young volcanic vent is less than 75 km than they do when the distance is greater than 75 km. The cause of this longer-distance correlation is unknown, but might be related to a tendency of young volcanic vents to define broader regional zones of crustal extension.

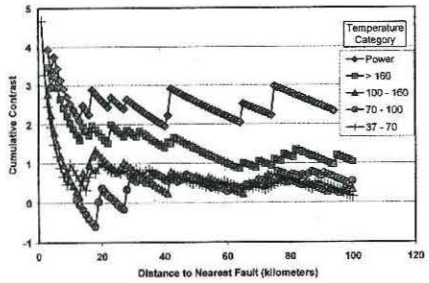

Figure 2. Cumulative weights-of-evidence contrast for geothermal training points vs. young volcanics ≤1.5Ma.

Young Faults

Previous investigators (Rowan and Wetlaufer, 1981; Koenig and McNitt, 1983) have noted that high-temperature geothermal systems in Nevada often occur along northeast-trending structures. That relationship is difficult to quantify visually on statewide structure maps (Figure 1b), but the weights-of-evidence contrast statistic (Table 1) provides clarification, showing that high-temperature and "power" systems correlate better with northeast-trending young (<1.5Ma) faults than lower-temperature systems. Furthermore, high-temperature systems correlate better with young northeast-striking faults than they do with either young northwest-striking faults or northeast-striking faults of all ages (Figure 3a). Lower-temperature systems appear to correlate better with northwest-trending young faults (Figure 3b).

Table 1. Weights-of-evidence statistics for northeast-trending faults, groundwater boron, and water table depth. Confidence equals contrast divided by its standard deviation.

EVIDENCE LAYER	Training Set	Positive Weight	Negative Weight	Maximum Contrast	Confidence
NE-Trending Faults	Power	2.33	-0.24	2.57	3.89
NE-Trending Faults	High Temp	2.20	-0.32	2.52	5.17
NE-Trending Faults	Med Temp	0.18	-0.75	0.93	1.94
NE-Trending Faults	Low Temp	1.14	-0.08	1.22	2.56
NE-Trending Faults	Warm	1.21	-0.06	1.27	2.43
Groundwater Boron	Power	4.00	-0.09	4.09	3.85
Groundwater Boron	High Temp	3.49	-0.05	3.54	3.40
Groundwater Boron	Med Temp	0.81	-0.34	0.95	2.67
Groundwater Boron	Low Temp	0.07	-1.29	1.36	1.35
Groundwater Boron	Warm	0.20	0.00	0.20	0.20
Water Table Depth:					
Water table in mountains assumed = 60m	High Temp	1.11	-1.95	3.06	4.11
Modeling not limited by physiography	High Temp	0.81	-2.27	2.68	2.81
Modeling limited to valleys only	High Temp	0.55	-2.11	2.66	2.58

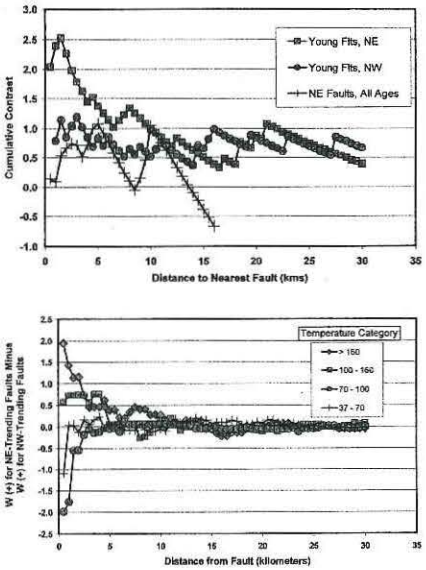

Figure 3. (a) Cumulative weights-of-evidence contrast of high-temperature geothermal systems relative to faults. The correlation is greatest between high-temperature systems and northeast-trending young faults. (b) Difference between cumulative positive weight-of-evidence in a northeast direction and cumulative positive weight in a northwest direction. High positive numbers indicate a preference for northeast-trending structures; high negative numbers indicate a preference for northwest-trending structures; values near zero indicate no preference. Within a distance of 5 km, high-temperature systems prefer northeast-trending structures.

These phenomena can be explained if northeast-trending structures remain open to greater depths than northwest-trending structures, allowing meteoric fluids to be heated to higher temperatures. Recent GPS-based crustal strain measurements (Bennett, *et. al.*, 1998) indicate that for much of Nevada, the principal strain direction is oriented northwesterly, suggesting that maximum extension rates occur on northeast-oriented faults. Higher rates of extension could translate to greater depths of fluid penetration along structures because higher strain rates push the brittle-ductile transition to greater depths (Fournier, 1999) and because hydrothermal mineral deposition otherwise continually works to seal open fractures. The sealing of fractures by hydrothermal minerals also explains why older inactive faults are more likely to host fossil, rather than active, geothermal systems.

For this paper, northeast-trending faults were actually defined as faults striking N62°E +/- 45°, perpendicular to a N28°W deformation direction for the Walker Lane and west and central Nevada described in an unpublished 2000 information sheet by R. A. Bennett and J. L. Davis. The direction of the GPS strain field actually varies across Nevada, becoming more nearly east-west in the eastern Great Basin (Bennett, *et. al.*, 1998). A more correct method of modeling the relationship between modern extension and geothermal activity would account for the change in strain direction and type of strain (shear or extension) with location; such an analysis is in progress (Blewitt, *et. al.*, 2002).

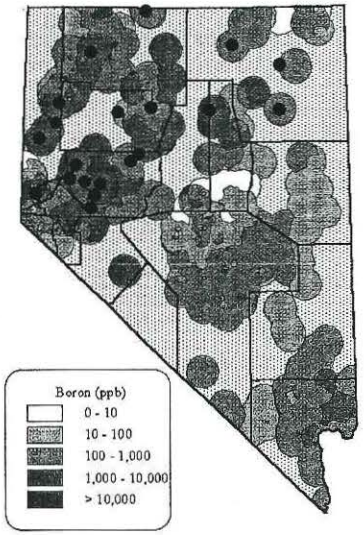

Figure 4. Modeled boron concentrations in groundwater. Black circles are high-temperature geothermal systems (>160°C). White dotted background represents areas with no data. Surface was contoured using log-normalized well and spring data from USGS NWIS database, using inverse distance weighting techniques.

Groundwater Chemistry

Contoured maps of boron in groundwater were interpolated from log-normalized trace element data from water wells and springs of the USGS NWIS database using inverse distance weighting methods. As expected, high-temperature geothermal systems correlate with high B concentrations (Figure 4, Table 1). A cause and effect relationship between geothermal activity and high groundwater B is further suggested by the fact that production fluids from geothermal power plants in Nevada have very high B concentrations. Analyses from 8 producing systems in Nevada average 13,700 ppb B (data from De Rocher, 2002). Though not shown here, lithium concentrations in groundwaters also correlate with geothermal activity; the correlation coefficient between B and Li in the NWIS database is 0.78.

Groundwater Depth

Koenig and McNitt (1983) observed that surface manifestations of geothermal activity are weak or absent where groundwater tables are deep. Undiscovered geothermal systems may occur in areas with deeper groundwater levels where hot springs aren't present to call attention to underlying geothermal activity.

Spatial analysis is consistent with the observations of Koenig and McNitt (1983). A significant weights-of-evidence contrast (Table 1) indicates that known high-temperature geothermal systems preferentially occur in areas where the depth to groundwater is 30 meters or less (Figure 5). Although most wells in the NWIS database are located in valleys and few are from mountain ranges, significant weights-of-evidence contrasts were obtained (Table 1) regardless of whether interpolation of the groundwater surface was 1) limited to valleys, 2) extrapolated into mountains, or 3) the mountains were assumed to have a water table depth of greater than 60 meters. Because of the potential significance groundwater levels have in geothermal exploration, detailed modeling of statewide groundwater tables is now in progress, incorporating basin geometries and well data from several additional sources.

Other Evidence Layers

Maximum weights-of-evidence contrasts for all evidence layers are listed in Table 2. Regional heat flux correlates positively with geothermal activity, as expected. Isostatic gravity highs tend to vary in concert with heat flux anomalies. Paleozoic carbonates in southern and eastern Nevada are less likely to host high-temperature geothermal systems than other rocks, probably because deep aquifers in carbonate rocks capture and entrain geothermal fluids rising from depth (Sass, *et. al.*, 1971). Earthquake frequencies and magnitudes also correlate with geothermal systems, although not as strongly as other evidence layers, in part because the time-span of seismograph measurements (<100 years) is short.

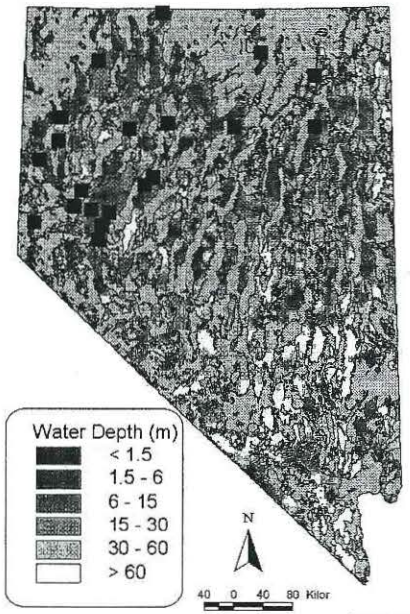

Figure 5. Depth to groundwater in Nevada, based on the USGS NWIS database. The background dotted pattern represents areas of "No Data", which are areas of non-Quaternary sedimentary rocks, occurring mostly in mountain ranges. Black squares are high temperature geothermal systems (>160°C).

Evidence layers with the highest contrasts, such as the water table depth and northeast-trending faults (Table 2) will have the greatest influence on predictive maps of geothermal potential. Evidence layers with lower contrasts, including heat flux and earthquakes, will have less influence.

Model Integration

A map predicting where high-temperature geothermal systems are most likely to occur was produced by combining seven of the eight evidence layers described above, using logistic regression. Gravity was not initially included as a layer because of its high correlation with regional heat flux. Favorable zones shown on the resulting map (Figure 6a) correlate well with the distribution of known high-temperature resources. There is, however, a limitation to this model, because it only predicts where geothermal systems are most likely to have already been found, and not necessarily where they are most likely to remain concealed.

Table 2. Weights-of-evidence statistics for evidence layers used in favorability modeling of high-temperature geothermal systems. Confidence equals contrast divided by its standard deviation.

EVIDENCE LAYER	Positive Weight	Negative Weight	Contrast	Confidence
Water Table Depth	1.11	-1.95	3.06	4.11
Isostatic Gravity	0.48	-2.12	2.60	2.53
NE Faults	2.20	-0.32	2.52	5.17
Boron	1.53	-0.50	2.03	4.50
Young Volcanics	1.68	-0.30	1.98	4.06
PZ Carbonates	0.33	-1.26	1.58	2.13
Heat Flux	0.47	-0.92	1.40	2.50
Earthquakes	0.59	-0.43	1.02	2.27

For exploration purposes, a better approach would focus predictions in areas where groundwater tables are deep, where a lack of surface hot springs or other thermal activity may belie an underlying geothermal system. A model was built using evidence unbiased with respect to the depth to the groundwater table. That evidence includes young volcanism, young faults, earthquakes, and, as a proxy for heat flow, regional isostatic gravity. This model compares well with the 7-layer model in areas where groundwater is shallow; much of the predictive power has been preserved even though only 4 evidence layers were used (Figure 6b).

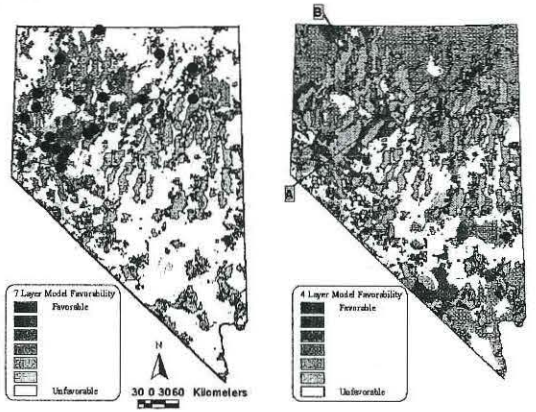

Figure 6. (a) Relative favorability for high-temperature geothermal systems based on 7-layer logistic regression model. Black circles are high-temperature (>160°C) geothermal systems. Black lines outline basin areas where water table is ≤30m. (b) Exploration favorability predicted by the 4-layer logistic regression model where the groundwater table is deeper than 30 meters. Background shaded dots indicate mountain ranges and/or where depth to water table is >30 meters. Points A and B are discussed in text.

Several interesting areas of relatively high exploration potential are indicated. One of these, the Stillwater Range west of Dixie Valley (point A, Figure 6b), is one of the few places in Nevada where an exploration well drilled near the crest of a range encountered thermal waters (Dick Benoit, personal communication, 2002). That well was not included in the training sites for modeling, though good favorability was predicted without it. A second area of interest lies near Denio, NV. (point B, Figure 6b). Favorable potential was predicted even though a high-temperature geothermal system at Borax Lake, Oregon, 40 km north of the state line, was not included as a training site because it fell outside the state of Nevada.

Conclusions

Spatial analysis with a GIS has helped quantify regional controls on extensional geothermal systems in Nevada. A relationship between high-temperature systems and northeast-trending structures, long-suspected, has now been quantified, and a possible link between geothermal activity and ongoing lithospheric plate motion is hypothesized. Extensional-type geothermal systems in Nevada reach high temperatures (>160°C) because of high heat flow and active extensional faulting (e.g., Wisian et. al., 1999), but other variables, including the presence of young volcanic vents (<1.5Ma), earthquakes, anomalous groundwater chemistry, and presence or absence of deep aquifers can be used to refine exploration models by combining these often used characteristics into one model.

Deep groundwater tables may conceal geothermal systems in some portions of the state because telltale hot springs may not be present. A logistic regression model was built to predict which areas of deep groundwater are most likely to host concealed geothermal resources, using the distribution of young faults, young volcanic rocks, isostatic gravity anomalies, and historical earthquakes as evidence. This predictive model could help increase the geothermal resource base by focusing exploration in the most prospective regions.

Acknowledgments

We are indebted to Mark Mihalasky, who constructed a prototype geothermal GIS and provided much of the digital data and initial encouragement to embark on this study. The support and assistance of the GBCGE, the USGS, the NBMG, and the Desert Research Institute are gratefully acknowledged. This research is based upon work supported by the U.S. Department of Energy under instrument number DE-FG07-02ID14311.

References

Bennett R.A., Wernicke B.P., and Davis J.L., 1998, Continuous GPS measurements of contemporary deformation across the northern Basin and Range Province; Geophysical Research Letters 25, 4, 563-566.

Blewitt, G., Coolbaugh, M.F., Holt, W., Kreemer, C., Davis, J.L., and Bennett, R.A., 2002, Targeting of potential geothermal resources in the Great Basin from regional relationships between geodetic strain and geological structures; (this volume)

Blackwell, D.D., 1983, Heat flow in the northern Basin and Range province; Geothermal Resources Council Special Report No. 13, p. 81-92.

Bonham-Carter, G.F., 1996, Geographic Information Systems for Geoscientists, Modelling with GIS: Elsevier Science Inc., Tarrytown, N.Y., 398 p.

De Rocher, T., 2002, The Geochemistry of the Productive Geothermal Systems in Nevada: Ph.D. dissertation in review, University of Nevada, Reno.

Edmiston, R.C. and Benoit, W.R., 1984, Characteristics of basin and range geothermal systems with fluid temperatures of 150° to 200° C; Geothermal Resources Council Transactions, v. 8, p. 417-424.

Fournier, R. O., 1999, Hydrothermal processes related to movement of fluid from plastic into brittle rock in the magmatic-epithermal environment: Econ. Geol. 94, 1193-1211.

Garside, L., 1994, Nevada low-temperature geothermal resource assessment: 1994; Nevada Bureau of Mines and Geology Open File Report 94-2.

Kemp, L.D., Bonham-Carter, G.F., Raines, G.L. and Looney, C.G., 2001, Arc-SDM: Arcview extension for spatial data modelling using weights of evidence, logistic regression, fuzzy logic and neural network analysis: http://ntserv.gis.nrcan.gc.ca/sdm/.

Koenig, J.B. and McNitt, J.R., 1983, Controls on the location and intensity of magmatic and non-magmatic geothermal systems in the Basin and Range province; Geothermal Resources Council Special Report No. 13, p. 93.

Mariner, R.H., Presser, T.S., and Evans, W.C., 1983, Geochemistry of active geothermal systems in the northern Basin and Range province; Geothermal Resources Council Special Report No. 13, p. 95-119.

Raines, G.L., Sawatzky, D.L., and Connors, K.A., 1996, Great Basin Geoscience Data Base; USGS Digital Data Series DDS-041.

Raines, G.L., Bonham-Carter, G.F., and Kemp, L., 2000, Predictive probabilistic modeling using ArcView GIS; ArcUser, v. 3, n. 2, p. 45-48.

Rowan, L.C. and Wetlaufer, P.H., 1981, Relation between regional lineament systems and structural zones in Nevada; Amer. Assoc. Petroleum Geologists Bull. v.65, n. 8, p. 1414-1432.

Sass, J.H., Lachenbruch, A.H., Munroe, R.J., Greene, G.W., and Moses, T.H.Jr., 1971, Heat flow in the Western United States; Jour. Geophys. Res. 76, 6376-6413

Shevenell, L., Garside, L.J., and Hess, R.H., 2000, Nevada Geothermal Resources; Nevada Bureau of Mines and Geology Map 126.

Singer, D.A., 1996, ed., An analysis of Nevada's metal-bearing mineral resources; Nevada Bureau Mines and Geology Open-File Report 96-2.

Wisian, K.W., Blackwell, D.D., and Richards, M., 1999, Heat flow in the western United States and extensional geothermal systems: Proceedings, 24th Workshop on Geothermal Reservoir Engineering, Stanford, CA., p. 219-226.

Wright, D.F., 1996, Evaluating Volcanic Hosted Massive Sulfide Favourability using GIS-Based Spatial Data Integration Models, Snow Lake Area, Manitoba: Ph.D. dissertation, Univ. Ottawa, 344 p. and CD-ROM with data.

Geologic Setting and Preliminary Analysis of the Desert Peak-Brady Geothermal Field, Western Nevada

James E. Faulds[1], Larry J. Garside[1], Gary L. Johnson[1], Jessica Muehlberg[2] and Gary L. Oppliger[2],

[1]Nevada Bureau of Mines and Geology and [2]Department of Geological Sciences
University of Nevada, Reno, NV 89557

Keywords

Nevada, geothermal, Desert Peak, Brady, Humboldt structural zone, faults

ABSTRACT

A broad heat-flow anomaly (Battle Mountain heat-flow high) parallels the northeast-trending Humboldt structural zone in northern Nevada. The Humboldt zone contains subparallel northeast-striking left-lateral and normal faults, as well as northeast-trending folds. Several major geothermal fields, including Desert Peak-Brady, Steamboat, Soda Lake, Rye Patch, Dixie Valley, and Beowawe, lie within the Humboldt structural zone. Although the northeast-striking faults are thought to control some of the geothermal fields, the exact links between the fields and structural and stratigraphic features are generally poorly understood.

We have undertaken an integrated geologic, geophysical, and GIS investigation of the Desert Peak-Brady geothermal field in the Hot Springs Mountains of western Nevada. Two power plants and one vegetable dehydration plant currently operate in this field. The Hot Springs Mountains are composed of Tertiary volcanic and sedimentary rocks that rest directly on Mesozoic metamorphic basement. Both northeast- and east-northeast-striking faults dissect the range. In addition, the Tertiary rocks (some of which are less than 9 Ma) are deformed into closely spaced open to tight northeast-trending folds. The Desert Peak-Brady field is found along a major northeast-striking fault zone that extends from near Fernley to Lovelock and essentially bounds the Carson Sink on the north. The Brady field (Brady's Hot Springs) follows the northeast-striking Brady fault. Evidence for both normal- and left-lateral slip has been found on the Brady fault. The Desert Peak field is a *blind* geothermal reservoir ~5 km (3 miles) southeast of Brady's Hot Springs. The Desert Peak reservoir resides in pre-Tertiary rocks. Available aqueous chemistry and isothermal maps suggest that the Brady and Desert Peak plants are associated with essentially independent thermal plumes. Isothermal maps also indicate a third thermal plume (Desert Queen) in the eastern Hot Springs Mountains approximately 8 km east-northeast of the Desert Peak plant. Overall, the geothermal anomaly in the Hot Springs Mountains appears to trend northeast, approximately parallel to the presumed fault zone on the northwest margin of the Carson Sink. We speculate that the three thermal plumes in the northern Hot Springs Mountains are related to small left steps or pull-aparts in a broad zone of oblique, left-lateral normal displacement.

Introduction

A broad region of high heat flow, the Battle Mountain heat flow high, covers much of northern Nevada and includes an east-northeast-trending zone extending from near Reno to Carlin (Figure 1). The Steamboat, Desert Peak-Brady, Soda Lake, Rye Patch, Dixie Valley, and Beowawe geothermal fields lie within this zone. Northeast-striking faults that roughly parallel the Battle Mountain high appear to host most of these geothermal fields. This belt of east-northeast- to northeast-striking faulting and high heat flow has been referred to as the Humboldt structural zone (Rowan and Wetlaufer, 1981). The abundance of producing geothermal fields and regional extent of the heat flow anomaly indicate high potential for discovery of additional geothermal reservoirs in this region. Despite the economic significance of the Humboldt zone, its structural and geophysical framework has not been comprehensively studied. Even with significant recent contributions (e.g., McNitt, 1990; Blackwell, *et. al.*, 1999; Caskey and Wesnousky, 2000), the temporal and spatial relationships between various structural features within the zone and how individual faults, stratigraphic units, or sets of structures control fluid pathways and geothermal resources are generally poorly understood.

We have recently undertaken an integrated structural, geophysical, geochronologic, and Geographic Information Systems (GIS) investigation of the Desert Peak-Brady geothermal field in the Hot Springs Mountains of western Nevada. Collectively,